Proceedings of 2013 IAHR Congress

Flow and Sediment Transport Through Bottom Racks. CFD Application and Verification with Experimental Measurements.

Luis Gerardo Castillo,
Professor, Dept. of Civil Engineering ,Universidad Politécnica de Cartagena, Spain. E-mail: luis.castillo@upct.es

José María Carrillo, Juan Tomás García,
PhD Student, Dept. of Civil Engineering ,Universidad Politécnica de Cartagena, Spain. E-mail: jose.carrillo@upct.es, juan.gbermejo@upct.es

ABSTRACT: Bottom rack intake systems are designed to get the maximum quantity of water in mountain rivers with important transport of sediments. Some attentions have been given to the occlusion of the racks due to the deposition of debris over them or to the quantity of sediments that gets into the racks and is transported along the derivation channel. Currently, we want to optimize this kind of intake systems to use them in discontinuous and torrential streams with high sediments concentrations.
Some experimental studies have found a correlation between the influence of the sediments and the flow derived by the rack (Orth et al., 1954). Krochin (1978) proposes an increment coefficient in the length of the rack for considering the clog problems. Drobir (1981) published some results for different types of sieve curves in mountain rivers.
The methodology of Computational Fluid Dynamics (CFD), which is based on numerical solution of the Reynolds Averaged Navier-Stokes (RANS) equations together with turbulence models of different degrees of complexity, simulates the interaction between different fluids, such as the sediment transport and the air-water two-phase flow that appear in the phenomenon of intake systems.
This paper compares and discusses the results obtained using a CFD numerical model with the experimental results obtained by Noseda (1956), Drobir (1981) and UPCT Lab.

KEY WORDS: Bottom intake system, Racks, Circular bars, Sediment, CFD.

1 INTRODUCTION

In the design of a bottom intake system, it is necessary to consider different aspects. The efficiency of the racks depends on various factors such as the shape of the bars, clear spacing between the bars (void ratio), flow approximation conditions and quantity, the angle of the rack, length, sediment rate, etc.

It is assumed that flux over the rack is one-dimensional, flow decreases progressively, hydrostatic pressure distribution acts over the rack in the flow direction and energy level or energy head can be considered constant along the rack.

Several researchers have studied this problem using hydraulic models. Noseda (1956) studied the clear water flow through different racks. Differences between measured and calculated depth profiles are generally found at the beginning of the rack due to the consideration of hydrostatic pressure distribution, and at the edge of the rack when friction effects are neglected (Brunella et al., 2003).

Righetti and Lanzoni (2008) proposed to calculate the flow derived by the rack with the following differential equation:

$$dq(x) = C_q m \sqrt{2g(H_0 + \Delta z)}dx \tag{1}$$

where m is the void ratio, dx is the differential rack length in the flow direction, H_0 is the total energy at the beginning of the rack, Δz is the vertical distance between the edge of the rack and the analyzed section, and C_q is the discharge coefficient. These authors proposed that $C_q \approx sin\ \alpha$, being α the angle between the velocity vector of water derived and the plane of the rack (see Figure 3).

Noseda (1956) defined a variable discharge coefficient for horizontal rack case and subcritical approximation flow:

$$C_q = 0.66m^{-0.16}\left(\frac{h}{l}\right)^{-0.13} \tag{2}$$

where l is referred to the inter axis (distance between the centerline of two consecutive bars), m is the void ratio and h is the height of water measured in the vertical direction. Once all the parameters are defined, several researchers (Frank, 1956; Bouvard and Kuntzmann, 1954; Noseda, 1956) have proposed the wetted rack length necessary to derive a defined flow rate. The value proposed by Noseda (1956) is obtained with the following equation:

$$L = 1.1848.\frac{E_0}{C_q m} \tag{3}$$

where L is the wetted rack length and E_0 is the specific energy at the beginning of the rack. In this way, Castillo and Lima (2010) analyzed and compared the formulae of wetted rack length obtained by several authors.

2 CLEAR WATER SIMULATION

2.1 UPCT Physical Model

An intake system has been constructed in the Hydraulic Laboratory at the Universidad Politécnica de Cartagena (Figure 1). The device is similar to Noseda´s model. It consists of a 5.00 m long and 0.50 m wide channel, a rack with different slopes, the discharge channel and the channel to collect water discharged. The racks are made of aluminum bars and were located at the bottom of the channel.

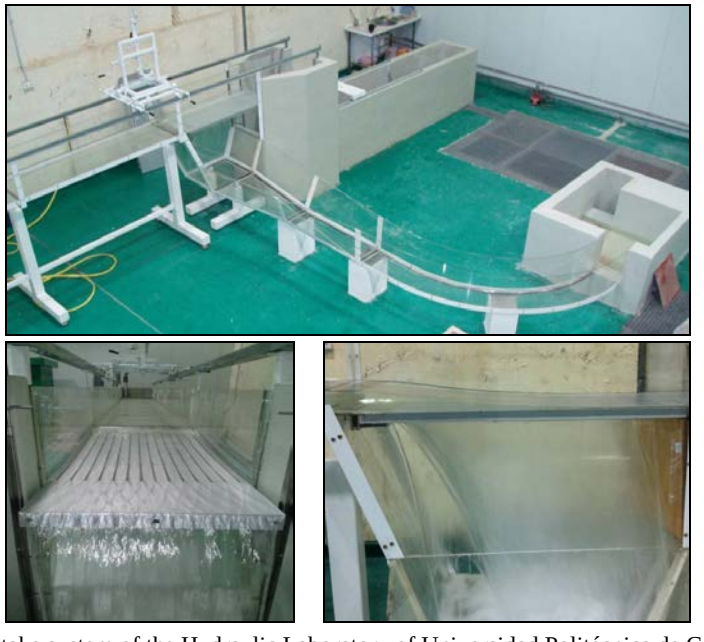

Figure 1 Device of intake system of the Hydraulic Laboratory of Universidad Politécnica de Cartagena, Spain

The experiments have been carried out using racks with different void ratios. The racks are built with *T* profile with the same width, but the longitudinal layout was modified to allow different spacing between them. Table 1 summarizes the geometric characteristics of each experiment that has been carried out.

Table 1 Geometric characteristics of the lab experiments

Experiment	A	B	C
Length, L (m)	0.900	0.900	0.900
Bar type (mm)	T 30/25/2	T 30/25/2	T 30/25/2
Direction of the flow	Longitudinal	Longitudinal	Longitudinal
Spacing, b_1 (mm)	5.70	8.50	11.70
Void ratio $m = \frac{b_1}{b_1 + 30}$	0.16	0.22	0.28

In each experiment, the incoming, derived and rejected flows and the longitudinal flow profile have been measured. q_1 is the incoming specific flow, q_2 is the specific discharge flow rejected, and q_d is the specific discharge flow derived from the intake system. Table 2 shows the entrance specific flow.

Table 2 Entrance specific flow in the intake system

Nº experiment	1	2	3	4	5
q_1 (l/s/m)	53.8	77.0	114.6	155.4	198.3

2.2 Drobir Physical Model

Drobir et al. (1999) measured the wetted rack length (horizontal projection) in a 1:10 scale model. The prototype rack was made with 0.10 m circular cross section bars, a spacing between the bars of 0.15 m, and a slope of 20%. Specific discharge flows from 0.25 to 2.00 m^2/s were analyzed.

Two different lengths were considered: L_1 is the horizontal projection of the distance where the surface of the nappe crossed the axis of the rack bar (measured between the bars), while L_2 is the maximum horizontal distance where the bars are wet (Figure 2).

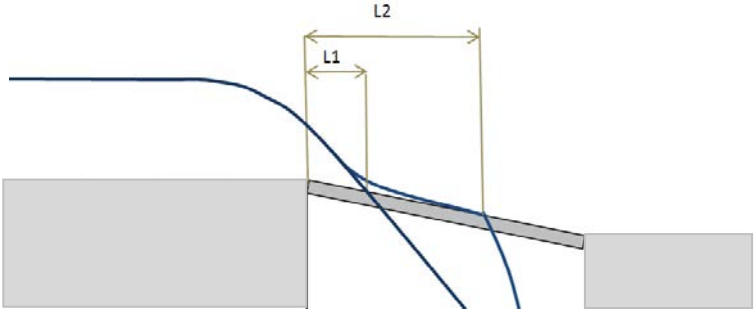

Figure 2 Scheme of wetted rack lengths L_1 and L_2 and shape of the nappe (Drobir, 1999)

In this paper the values measured by Drobir in their model have been compared to the wetted rack lengths calculated according to the methods of Bouvard and Kuntzmann (1954), Frank (1956) and Noseda (1956). All of these methodologies have been applied using the discharge coefficient formulation, C_q (equation 2). This is discussed in the epigraph 2.4.2.

2.3 Numerical Model

The Computational Fluid Dynamics programs allow us to simulate the interaction between different fluids as a two-phase air-water or flows with different concentrations, like sediment transport. This programs solve the fluid mechanical problems into its geometric configuration, providing lot of data, increased profitability, flexibility and speed compared with experimental procedures. However, to use them correctly, it is necessary to contrast and to calibrate numerical results with data obtained in prototypes and/or physical models.

To test the hydraulic behavior of an intake system simulation, the experimental data measured by Drobir et al. (1999), Noseda (1956) and Castillo et al. (2013) were used.

FLOW-3D uses a difference finite scheme, solving the differential Navier-Stokes equations of the phenomenon in control volumes defined by the meshing of the fluid domain. The continuity and momentum Navier-Stokes equations are applied:

$$\frac{\partial u_i}{\partial x_i} = 0 \tag{4}$$

$$u_j \frac{\partial u_i}{\partial x_i} = -\frac{1}{\rho}\frac{\partial}{\partial x_i}(P\delta_{ij} + \rho\overline{u_i u_j}) \tag{5}$$

being P the dynamic pressure, ρ the flow density, u_i the i component of the local time-averaged flow velocity, δ the Kronecker Delta function and $\rho\overline{u_i u_j}$ the turbulence stresses.

To complement the numerical solution of Reynolds equations and average Navier-Stokes (RANS), a turbulence model has been used. So, in this study was applied the Renormalization-Group (RNG) k-ε model (Yakhot and Orszag, 1986; Yakhot and Smith, 1992). This turbulence model applies statistical methods to the derivation of the averaged equations for turbulence quantities. The RNG model is known to describe flows having strong shear regions more accurately than the k-ε standard model (FLOW-3D, 2011).

To simulate clean water flow, we selected the one fluid option, join to the air entrainment models. Figure 3 shows the velocity vectors and the angle α between the velocity vector of water derived and the plane of the rack.

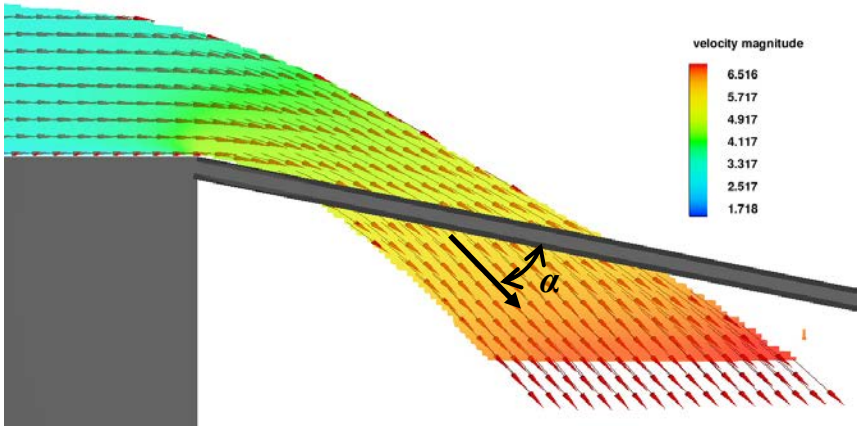

Figure 3 Free surface and velocity field of clean water passing through the rack, considering upstream subcritical condition and q = 1.00 m^3/s/m

The model boundary conditions correspond to the flow at the inlet condition, the upstream and downstream levels and their hydrostatic pressure distributions. Outflow conditions were used at the bottom of the exit channel of water collected due to the fact that at this boundary the hydrostatic pressure condition is not exist.

For simplicity, it was considered that all the longitudinal bars work in the same mode in the intake system (Castillo and Carrillo, 2012). For that reason, a model with six bars and five spacing, with symmetrical conditions in the longitudinal boundaries of the fluid domain has been considered. The mesh was obtained using a regular mesh size of 0.008 m in our lab model and 0.025 m in Drobir model (Figure 4).

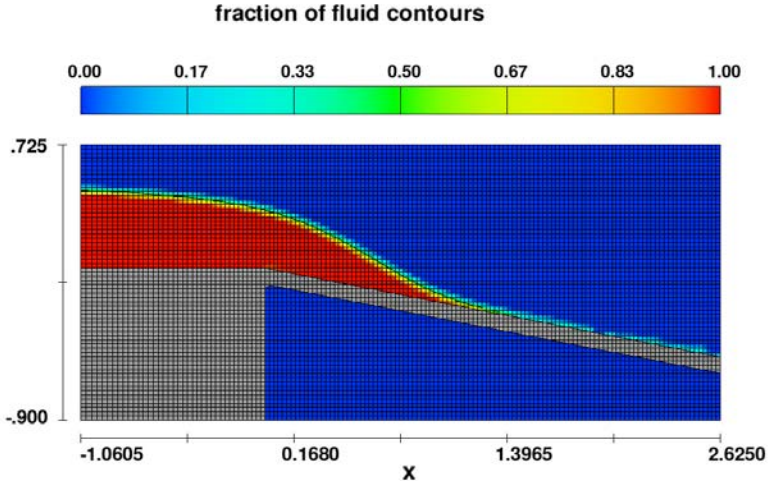

Figure 4 Detail of the mesh size and the flow passing over a bar for clean water considering Drobir model. Upstream subcritical condition and q = 1.00 m^3/s/m

2.4 Results and Discussion

2.4.1 UPCT physical model

In order to know the accuracy of the numerical simulations data, the longitudinal flow profiles over the centre of the bar simulated we compared with the results obtained by Noseda (1956) and UPCT laboratory.

Figure 5 compares the depth of the longitudinal flow profiles (horizontal rack) obtained with the biggest, medium and smallest specific flows, using the three methodologies and considering spacing b_1=11.70 mm (m = 0.28). In general, the water profiles obtained with CDF methodology are similar to the lab measurements. In the central part of the rack, the differences of FLOW-3D are up to 15% below of Noseda depth when the bigger specific flow is considered.

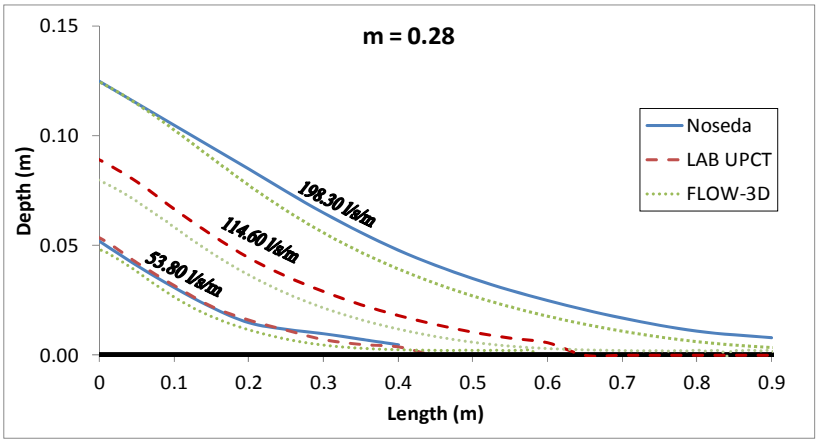

Figure 5 Flow profiles over the centre of the bar with horizontal rack, b_1 = 11.70 mm and q_1 = 53.8, 114.6 and 198.30 l/s/m

The relation between specific flow, q_1, and specific flow derived in the intake system, q_d, for spacing b_1 = 11.70 mm has been also compared. Figure 6 shows similar results with lab and Noseda´s measurements, except for q_1=198.3 l/s/m in which FLOW-3D collected more flow.

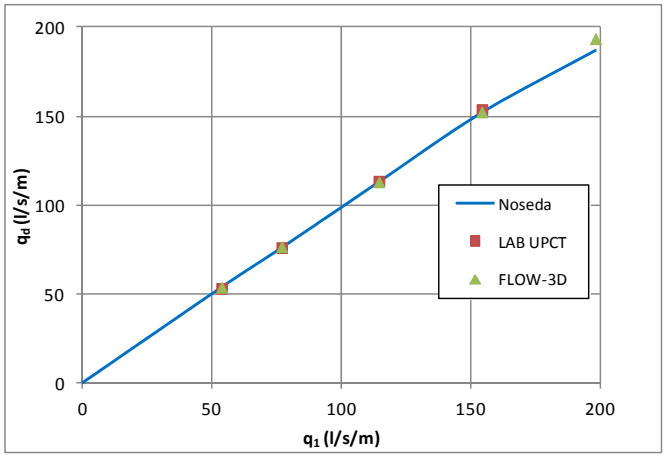

Figure 6 Derivation capacity of the intake system, with b_1 = 11.70 mm (m = 0.28)

The comparison of the results obtained with FLOW-3D with the lab results measured by Noseda (1956) and in the laboratory of the Universidad Politécnica of Cartagena show a satisfactory accuracy between them and validates this model for the case of clean water (Castillo and Carrillo, 2012).

2.4.2 Drobir physical model

In order to know the accuracy of the numerical simulations data with sloped circular bars, in Figure 7, longitudinal profiles of flow simulated by CFD are presented for the same rates that Drobir measured in his model, considering subcritical flow. From these graphs, the wetted rack lengths L_1 and L_2 simulated can be obtained.

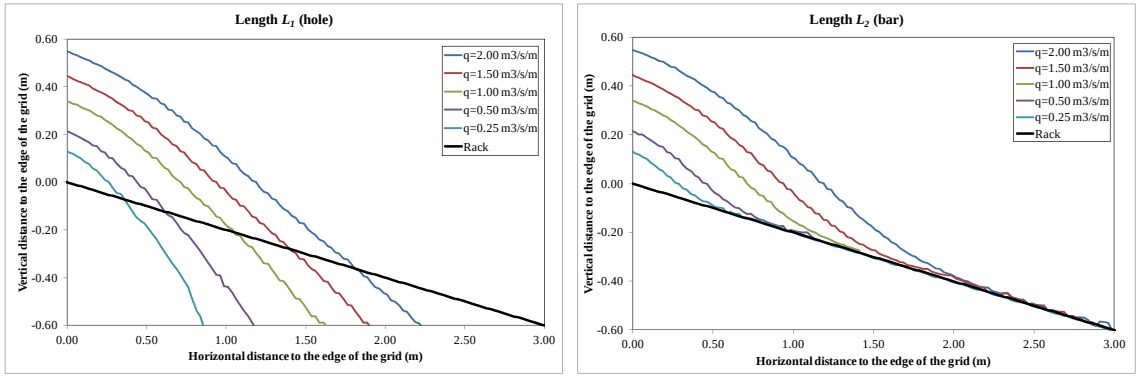

Figure 7 Water longitudinal profiles for a 20% slope rack, m = 0.60, considering different flow rates

Figure 8 shows the wetted rack lengths L_1 and L_2 simulated for different specific flows. In general, a good approximation can appreciate for both lengths. For the bigger flows, the L_1 length calculated with CFD tends to be bigger than the values of Drobir and the free overfall too. L_2 has a tendency to be a little smaller than Frank, Bouvard and Kuntzmann, Noseda and Drobir results. One of the causes of the differences can be due to the fact that the FAVOR method used by FLOW-3D to obtain the solid parts in the volume of fluid has difficulties to reproduce the shape of the circular bars, requiring a very fine mesh size. In this way, the smaller L_2 simulated can be also as a result of the difficulty to reproduce the smaller depths (less than 0.01 m) over the racks with the mesh size used (0.025 m). However, it is necessary to

taking into account that the use of a smaller mesh size increments the computational effort.

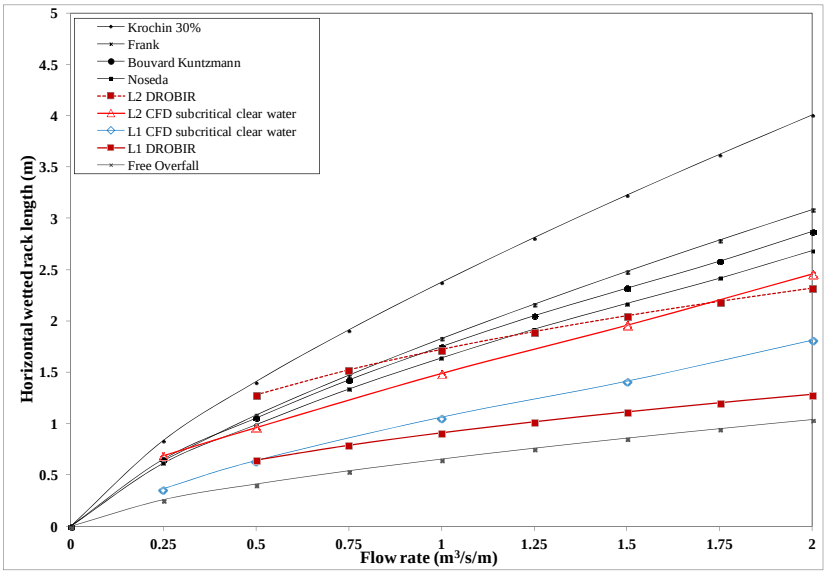

Figure 8 Wetted rack lengths (horizontal projection) for a 20% slope rack, m = 0.60, considering flow rates from 0.25 to 2.00 $m^3/s/m$

3 SEDIMENTS SIMULATIONS

3.1 Physical Model

Noseda (1956) did not considered sediments transport. However, some studies were carried out in the Drobir (1981) model. This model has been used to compare the numerical simulations when different concentration sediments are considered.

3.2 Numerical Model

In FLOW-3D, the sediments models consider two situations: lifting and particle transport. The first takes place at the interface between the liquid and the solid surfaces and generates the transport of the particles when the effort caused by the flow exceeds a critical value, and consequently, the amount of raised particles of the ground is proportional to the shear stress. The transport component simulates the movement of the solid particles in the fluid, and additionally, the model incorporates a drive module, which is used to simulate the behavior of solids when flowing at high concentrations. The density and viscosity of the fluid are calculated from the concentration of sediments.

3.3 Sediments Characteristics

For the sediments simulations, a constant diameter sediment has been used. The characteristic diameter was the defined by Sommer (cited by Drobir, 1981), who considered a sand whose d_{95} = 60 mm. Different volumetric concentrations between 1 and 5% have been simulated at the beginning of the rack.

3.4 Results and Discussion

In each simulation, the wetted lengths L_1 and L_2 have been calculated and compared with the values of clear water, when the inlet volumetric concentration of solids is varied. The flow rates simulated correspond to 1.00, 1.24 and 1.36 $m^3/s/m$. This specific flows match with the deduced by Hofner (Drobir, 1981) when measured the volume of sediments retained in a sand trap situated at the end of the rack.

In the physical model, Drobir (1981) considered that practically all the solid material enter in the rack due to the space between the bars of the rack, 0.15 m (void ratio, m = 0.60).

Due to the huge spacing between bars in the Drobir model, also it has been analyzed the sediment transport over the rack considering spacing between bars of 0.06 and 0.03 m (void ratios of m = 0.375 and 0.23 respectively). It has been considered subcritical and supercritical approximation regime at inlet boundary condition.

Figure 9 shows the water longitudinal profiles obtained with clean water and with 5.00 % of sediments concentration at the beginning of the rack, considering a 1.36 $m^3/s/m$ specific flow. The sediment transport tends to increment the depth over the bars and in the spacing between bars. Besides this, an increment in L_1 and L_2 can be observed.

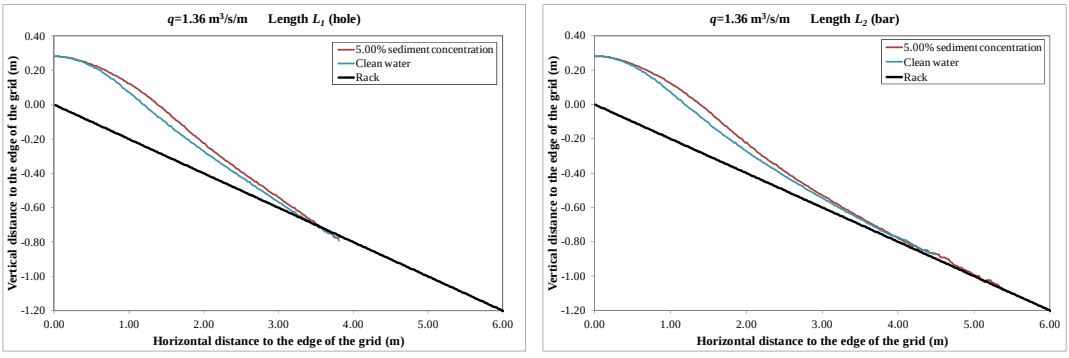

Figure 9 Water longitudinal profiles with clean water and 5.00 % sediment concentration, for q = 1.36 $m^3/s/m$, a 20% slope rack and m = 0.23

Figure 10 shows the horizontal wetted rack length considering a spacing between the bars of 0.15 m. When different sediment rates are considered, the wetted rack length simulated increases over the clean water case and those measured by Drobir et al. (1999), reaching increments of around the 20% respect to the initial L_2 length.

In the cases of supercritical flow approximation, the wetted lengths simulations with sediments also present increases respect to the simulation with subcritical flow approximation.

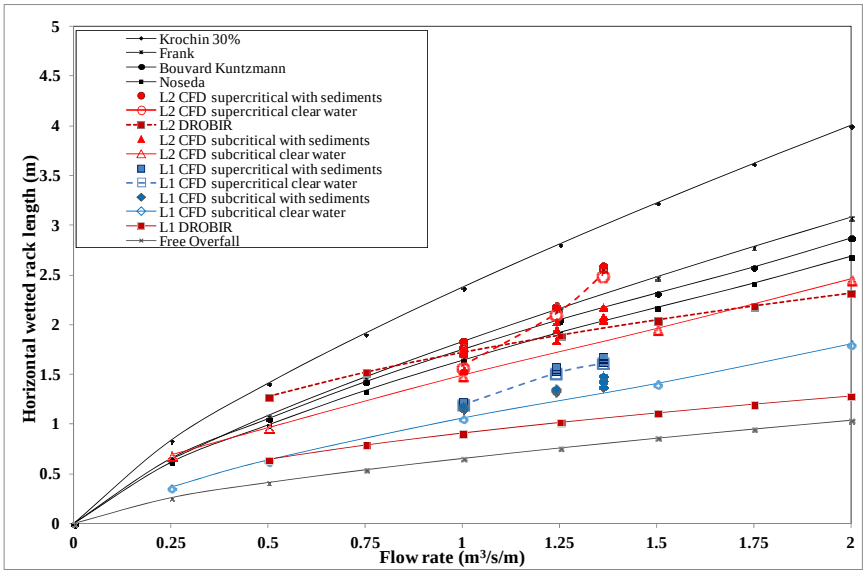

Figure 10 Wetted rack lengths (horizontal projection) for a 20% slope rack, m = 0.60, considering different flow rates (1.00, 1.24 and 1.36 $m^3/s/m$) and solid concentrations in volume (1.00, 2.50 and 5.00 %)

Figures 11 and 12 show the results for racks with void ratios of m = 0.375 and m=0.23 respectively. The wetted rack length increases with the volume concentration of sediments, maintaining the results found before. It also appreciates that the wetted lengths, L_1 and L_2, calculated with the CFD simulations with this void ratios give lower wetted lengths than those obtained with the methodology of Noseda (1956) (formulation for T-shaped horizontal bars and clean water). This can be a result of considering the shape of the bars (circular) in the CFD simulations, and therefore the increases of the discharge coefficient with the decreases of the void ratio. It is necessary to take into account that the program did not reproduce the clogging due to the sediments passing through the racks.

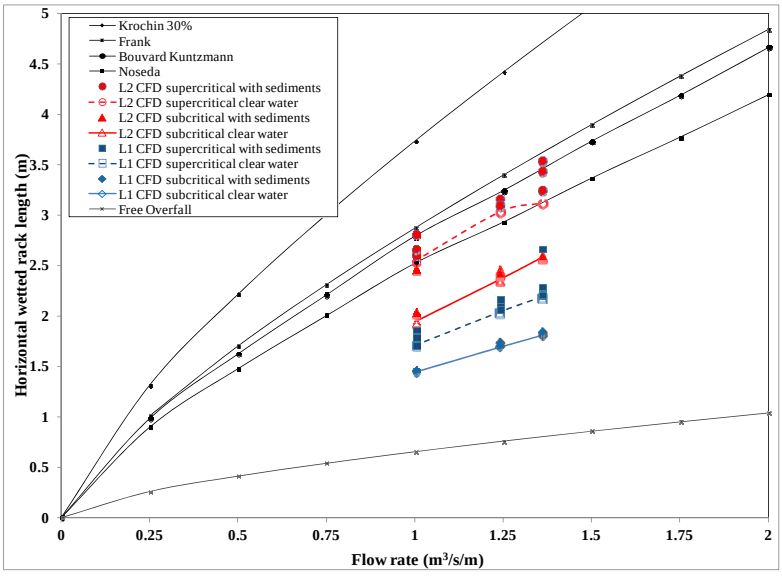

Figure 11 Wetted rack lengths (horizontal projection) for a 20% slope rack, m = 0.375, considering different flow rates (1.00, 1.24 and 1.36 $m^3/s/m$) and solid concentrations in volume (1.00, 2.50 and 5.00 %)

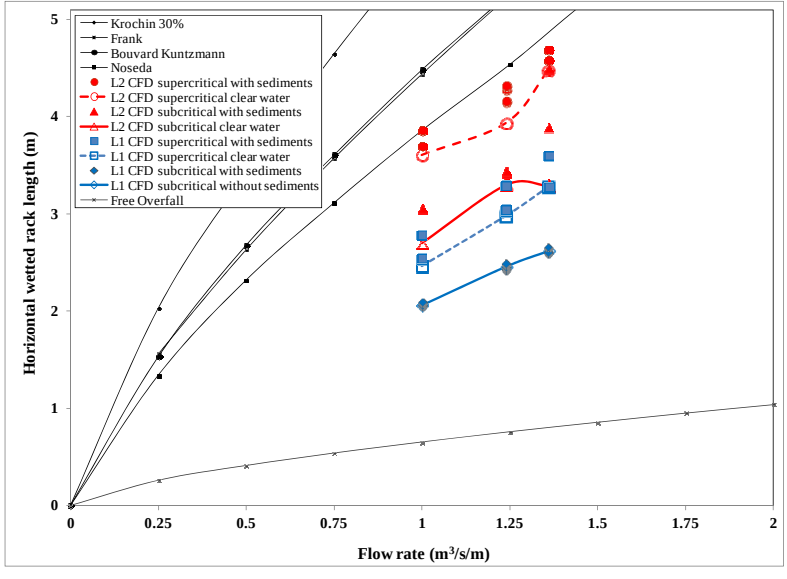

Figure 12 Wetted rack lengths (horizontal projection) for a 20% slope rack, m = 0.23, considering different flow rates (1.00, 1.24 and 1.36 $m^3/s/m$) and solid concentrations in volume (1.00, 2.50 and 5.00 %)

4 **CONCLUSIONS**

There are different laboratory studies modeling clean water flows over racks with different bar shapes, slopes and spacing. However, there are very few studies looking at the effects of sediment on the rack behavior.

To improve the knowledge of these structures, it is important to do more experimental studies, both in physical models and in prototypes, simultaneously measuring depths, velocity and sediment rates.

In this paper we have tested the accuracy of the numeric results obtained with CFD methodology as a tool to model an intake system, considering clean water. Furthermore, a numerical sediments preliminary study has been carried out.

Simulations do not reproduce the clogging due to the sediments passing over the racks, although the wetted rack length is increased due to the conditions of flow containing sediments.

The type of approximation flow influences on the wetted rack lengths, so it is recommended to consider supercritical and subcritical approximation flows when wetted rack lengths are analyzed.

Lab results will allow us to calibrate and validate the CFD code, not only with clean water, but also with sediments transport.

References

Bouvard, M., 1953. Debit d'une grille par en dessous. La Houille Blanche (in French).

Bouvard, M. and Kuntzmann, J., 1954. Étude théorique des grilles de prises d'eau du type. En dessous. La Houille Blanche (in French).

Bouvard, M., 1992. Mobile Barrages and Intakes on Sediment Transporting Rivers. IAHR Monograph. Series by A. A. Balkema, PO Box 1675, 3000 BR Rotterdam, The Netherlands.

Brunella, S., Hager, W. and Minor, H., 2003. Hydraulics of Bottom Rack Intake. ASCE Journal of Hydraulic Engineering, 129(1), 2-10.

Castillo, L.G. and Lima, P., 2010. Análisis del dimensionamiento de la longitud de reja en una captación de fondo. Proceedings of the XXIV Congreso Latinoamericano de Hidráulica, Punta del Este, Uruguay (in Spanish).

Castillo, L. & Carrillo, J.M., 2012. Numerical simulation and validation of intake systems with CFD methodology. Proceedings of the 2nd IAHR European Congress. Munich, Germany.

Castillo, L.G., Carrillo, J.M. and García, J.T., 2013. Comparison of clear water flow and sediment flow through bottom racks using some lab measurements and CFD methodology. Seven River Basin Management. Wessex Institute of Technology, New Forest, UK.

Drobir, H., 1981. Entwurf von Wasserfassungen im Hochgebirge. Österreichische Wasserwirtschaft, Heft, 11(12) (in German).

Drobir H., Kienberger, V., and Krouzecky, N., 1999. The wetted rack length of the Tyrolean weir. IAHR- Proceedings of the 28th Congress, Graz, Austria.

FLOW Science, Inc., 2011. FLOW 3D. Theory v10.0.

Frank, J., 1959. Fortschritte in der hydraulic des Sohlenrechens. Der Bauingenieur, 34, 12-18 (in German).

Frank, J., 1956. Hydraulische Untersuchungen für das Tiroler Wehr. Der Bauingenieur, 31, Helf 3. 96-101 (in German).

Krochin, S., 1978. Diseño Hidráulico. Segunda Edición. Colección Escuela Politécnica Nacional. Quito. Ecuador (in Spanish).

Noseda, G., 1956. Correnti permanenti con portata progressivamente decrescente, defluenti su griglie di fondo. L'Energia Elettrica, 565-581 (in Italian).

Orth, J., Chardonnet, E. and Meynardi, G., 1954. Étude de grilles pour prises d'eau du type. La Houille Blanche, 9(6), 343-351 (in French).

Righetti, M., Rigon, R. and Lanzoni, S., 2000. Indagine sperimentale del deflusso attraverso una griglia di fondo a barre longitudinali. Proceedings of the XXVII Convegno di Idraulica e Costruzioni Idrauliche, 3, Genova, Italy, 112–119 (in Italian).

Righetti, M. and Lanzoni, S., 2008. Experimental Study of the Flow Field over Bottom Intake Racks. ASCE Journal of Hydraulic Engineering, 134(1), 15-22.

Yakhot, V. and Orszag, S.A., 1986. Renormalization group analysis of turbulence. I. Basic theory. Journal of Scientific Computing, 1(1), 3-51.

Yakhot, V. and Smith, L.M., 1992. The renormalization group, the ε-expansion and derivation of turbulence models. Journal of Scientific Computing, 7(1), 35-61.